scientific reports

OPEN

Employing computational fluid dynamics technique for analyzing the PACK-1300XY with methanol and isopropanol mixture

Y. Cao[1], H. A. Dhahad[2✉], A. Khandakar[3], M. E. H. Chowdury[3], M. A. Ayari[4], S. M. Alizadeh[5] & B. Vaferi[6✉]

In this study, an innovative wire gauze structured packing, namely PACK-1300XY with a specific surface area of 1300 m²/m³ has been characterized by performing computational fluid dynamics (CFD) approach. Indeed, different features of this packing (height equivalent to a theoretical plate, wet/dry pressure drop, and mass transfer efficiency) were analyzed by analyzing the flow regime using the three-dimensional CFD approach with the Eulerian–Eulerian multiphase scenario. The results showed the mean relative deviation of 16% (for wet pressure drop), 14% (for dry pressure drop), and 17% (for mass transfer efficiency) between the CFD predictions and experimental measurements. These excellent levels of consistency between the numerical findings and experimental observations approve the usefulness of the CFD-based approach for reliable simulation of separation processes.

Separation technologies, like ionic liquid-based[1,2] and microvaiwe assisted[3] absorption, adsorption[4–7], membrane[8], circulating purification[9], and fluidizedization[10–12] have a wide ranges of application in different applications. The distillation column is likely the most well-known process to separate either feedstock and product stream by considering the relative volatility[13–15]. The distillation column can easily handle a counter-current flow regime between gas and liquid streams[16]. The distillation columns equipped with the tray[17] and packing[18] are two main categories in this regard. The latter is divided into two random and structured packings[19].

Because the structure packing has a wide range of benefits, including providing low-pressure drop, having high separation efficiency, and being adaptable with the different operations[20], it has been selected for the large-scale separation towers[21] and domestic chemical industries. In order to elaborate on the separation performance of the chemical procedures, one kind of structured packings, i.e., corrugated sheet packing, is popular[22]. Their material could be metals, ceramics, and plastics[23] arranged side by side with reverse canal directions. Therefore, their porosity is about ninety percent, with an attractive specific surface area ranging from 250 to 750 m²/m³[24].

The dry and wet pressure drops in the distillation columns are associated with the gas phase and the counter-current gas–liquid stream across the column height, respectively[25]. Moreover, the height equivalent to a theoretical plate (HETP) and liquid hold up are other essential characteristics of a packing[26,27]. Moreover, the separation efficiency for the packed bed has been defined via the HETP-value, which shows the mass transfer of packings. It should be noted that there is a proportional relation between these parameters[28].

Among the numerical studies for the fluid flow throughout the packings, computational fluid dynamic (CFD) is an efficient method to reduce the economic expense of experimental measurements[29–32]. Moreover, another benefit of this computational method is the capability of estimation for the effect of diverse factors[33–35]. To serve this purpose, several researchers developed precise discretization methods and the solution algorithms, i.e., providing an effective computational scheme, to introduce an accurate model for the simulation of the flow in the packings which the combination of in-house scripts and software would be used to this end[36].

In recent years, an enrichment of components at the gas–liquid interface[37,38] on the atomistic scale has an important influence on mass transfer mechanisms[39–41]. Moreover, several CFD-based studies have investigated

¹School of Mechatronic Engineering, Xi'an Technological University, Xi'an 710021, China. ²Mechanical Engineering Department, University of Technology, Baghdad, Iraq. ³Electrical Engineering Department, Qatar University, Doha, 2713, Qatar. ⁴Civil and Architectural Engineering Department, College of Engineering, Qatar University, Doha, 2713, Qatar. ⁵Petroleum Engineering Department, Australian College of Kuwait, West Mishref, Kuwait. ⁶Department of Chemical Engineering, Shiraz Branch, Islamic Azad University, Shiraz, Iran. ✉email: 10592@uotechnology.edu.iq; behzad.vaferi@gmail.com

the multiphase flow behavior of differently structured packings[42–45]. Moreover, the study of the empirical representation for commercial use of corrugated packings sheets has been presented in other computational works[46,47].

Amini et al. fabricated different wire gauze structured packings with the specific surface area range from 860 to 2100 m²/m³[48–50]. They observed a low-pressure drop for both dry and wet streams, low HETP, high specific surface area, and high liquid holdup for the fabricated packings. They also investigated the effect of different operational conditions on the performance of these structured packings employing the multiphase flow simulations.

Liu and co-workers performed the three-dimensional single-phase CFD simulations to study the behavior of the rotary packed bed (RPB) equipped with the wire mesh structured packing from stainless steel[51]. They studied the pressure, pressure drop, and gas flow profiles around the packing as a function of gas flow rate and rotational velocity. Moreover, by using the analysis of the gas flow behavior and pressure distribution and CFD method, they studied the geometry optimization of packing and RPB. It should be noted that several researchers focused on the simulation of the two-phase flow[52] and mass transfer in the interface of the structured packings[53].

Some efforts were also made to modify the current models and increase the calculation accuracy of the liquid holdup and pressure drop in the structured packings[54] and mass transfer evaluation[55]. Van Baten and Krishna investigated the mass transfer behaviors of the gas and liquid in a katapak-S packing[54]. They reported a good agreement between their results and the theoretical correlation presented by Viva et al.[56]. In addition, Manh et al. by using CFD simulation calculated the dry and wet pressure drop and mass transfer efficiency in the new structured packing[57]. The authors proposed a model near to the real geometry. The simulation results were in good agreement with experimental data[57].

This computational study aims to characterize a newly fabricated wire gauze structured packing employing the CFD approach. Another goal is the evaluation of this packing under different operating conditions. Furthermore, the CFD technique helps analyze the HETP, mass transfer efficiency, and wet and dry pressure of this new structured packing. In this approach, CFD characterizes the new structured packing (PACK-1300XY) using the isopropanol/methanol mixture.

Simulation details

Hydrodynamics. The flow geometry of the Newtonian/incompressible fluid inside the column in the isothermal condition has been simulated using the multiphase flow Eulerian/Eulerian model[58]. It should be noted that all the fluid-related characteristics are assumed to have constant behavior across the column height.

Moreover, the following equations are used to calculate the mass and momentum conservation laws in a volume-averaged mode, respectively[59–62].

$$\frac{\partial}{\partial t}(\gamma_\alpha \rho_\alpha) + \nabla(\gamma_\alpha \rho_\alpha U_\alpha - \Gamma_\alpha \nabla \gamma_\alpha) = 0 \quad \alpha = L, G \tag{1}$$

$$\frac{\partial}{\partial t}(\gamma_\alpha \rho_\alpha U_\alpha) + \gamma_\alpha \left\{ \rho_\alpha U_\alpha U_\alpha - \left[\mu_{e\alpha} \left(\nabla U_\alpha + (\nabla U_\alpha)^T \right) \right] \right\} = \gamma_\alpha (B_\alpha \nabla P) - F_\alpha \quad \alpha = L, G \tag{2}$$

where ρ, γ, μ and U are the fluid density, the occupied volume fraction by phases, the dynamic viscosity, and the interstitial velocity, respectively. In addition to these parameters, Γ indicates the volume fraction dispersion factor, μ_e and F_α designate the effective viscosity and the interfacial drag force, respectively.

Mass transfer behavior. The following equation was used to calculate the mass transfer relation:

$$\frac{\partial}{\partial t}(\gamma_\alpha \rho_\alpha Y_{i\alpha}) + \nabla[\gamma_\alpha (\rho_\alpha U_\alpha Y_{i\alpha} - \Gamma_\alpha \nabla Y_{i\alpha})] = \sum_{\substack{\beta = 1, \\ \beta \neq \alpha}}^{N} m_{\alpha\beta}^i \tag{3}$$

$$\alpha = 1, \ldots, N, \quad \beta = 1, \ldots, N_C$$

where N and N_C show numbers of phase and numbers of phase ingredients, respectively. Furthermore, Y is the weight fraction of the ith ingredient in a specific phase. $m_{\alpha\beta}^i$ indicates the transferred mass per unit volume per unit time of the ith ingredient from phase β to phase α. It is obvious that the weight fraction must satisfy the following equation:

$$\sum_{i=1}^{N_c} Y_i = 1 \tag{4}$$

Equation (5) presents the theoretical basis of calculating the $m_{\alpha\beta}^i$ using the two-film theory. This equation states that the summation of the gas (γ_G) and liquid (γ_L) phase volume fractions are equal to one:

$$\gamma_G + \gamma_L = 1 \tag{5}$$

where

$$\gamma_G = \frac{V_G}{V_G + V_L} \tag{6}$$

$$\gamma_L = \frac{V_L}{V_G + V_L} \tag{7}$$

Mass transfer in the interphase region. It is necessary to highlight that the interphase mass transfer, which several researchers have adequately described, is used in this regard[63].

Mass transfer efficiency. A Series of theoretical stages were used to predict the HETP value as follows[63]:

$$\text{HETP} = \left[\frac{\ln \lambda}{\lambda - 1} \right] H_{OG} \tag{8}$$

$$\text{H}_{OG} = H_G + \lambda H_L = \frac{U_{GS}}{k_G a_e} + \lambda \frac{U_{LS}}{k_L a_e} \tag{9}$$

$$\lambda = \frac{m}{L/G} = \frac{\alpha}{[1 + (\alpha - 1)x_A]^2} \cdot \frac{G}{L} \tag{10}$$

where λ shows the equilibrium per operation line slopes. Other parameters (k_G, k_L, and a_e) are directly achieved from the proposed model by Bravo et al.[16].

Turbulent flow. Because we deal with complication flow characteristics inside the structured packing, utilizing the turbulent model to obtain reliable results is inevitable. Therefore, the literature review approved that the 'Standard' $k - \omega$ model proposed by Wilcox is a suitable turbulent model for our considered case[64,65]. Moreover, this model provides a reliable prediction for the flow characteristic by considering the near-wall treatment for a small Reynolds number[66–69].

One of the advantages of the $k-\omega$ formulation is the near wall treatment for low-Reynolds number computations. The model does not involve the complex non-linear damping functions required for the k–ε model and is therefore more accurate and more robust. A low-Reynolds k–ε model would typically require a near wall resolution of $y^+ < 0.2$, while a low-Reynolds k–ω model would require at least $y^+ < 2$. In industrial flows, even $y^+ < 2$ cannot be guaranteed in most applications and for this reason; a near wall treatment needs to be used. It allows for a smooth shift from a low-Reynolds number form to a wall function formulation. The k–ω model assumes that the turbulence viscosity is linked to the turbulence kinetic energy and turbulent frequency via the relation:

$$\mu_t = \rho \frac{k}{\omega} \tag{11}$$

## The packing geometry and numerical simulation

Among the steps of CFD simulations, the most crucial one is related to preparing a suitable grid with acceptable precision[70,71]. For serving this purpose, a well-defined three-dimensional geometry with a proper number of elements is first constructed. Moreover, in this study, twelve packing sheets are simulated inside a cylindrical system. To better understand, the computational geometry of the structured packing have been illustrated in Fig. 1.

This study uses a wire gauze made from metal sheets to fabricate the structured packing known as PACK-1300XY. This packing was introduced by Dinh Manh et al.[72]. Also in this research, we used the experimental data that was published[72]. The specific area and porosity are 1300 m^2/m^3 and 0.91, respectively. It should be stated that this structured packing is regarded as a class of the Y-type and X-type with the corrugation angle of 45° and 60°, respectively. The PACK-1300XY constructed 12 sheets, six sheets with corrugation angles 60° and 45°. The completed details of PACK-1300XY are presented in Table 1.

To elaborate on the accuracy of our results, we have employed the 3D tetrahedral cell. In addition, to verify the independence between the grid and HETP, several different mesh densities, including 1,520,000, 3,520,000, 5,230,000, and 13,680,000, have been used, see Table 2. This table confirms a slight improvement in the relative error (~1%) by reducing the element size from 0.2 to 0.1 mm. Consequently, 0.2 mm seems a proper element size for discretizing the model.

Two-phase flow mass transfer efficiency, dry/wet pressure drop, and isopropanol/methanol binary mixtures are investigated during the hydrodynamic inspection of the considered packing. The properties of this binary system have been presented in Table 3. By considering these parameters, at the top section of the column, we set the inlet velocity for the boundary condition and the pressure outlet in the outlet condition. It should be noted that careful considerations should be applied for the correct values for volume fraction, mass fraction of the methanol in each phase, turbulent quantities, and velocity component at the boundary conditions. Indeed, no-slip boundary conditions at the wall, $k - \omega$ turbulent model was used for both gas and liquid streams.

The SIMPLE (semi-implicit method for pressure-linked equations) algorithm (the finite volume method) is used to compute the coupling between the pressure and velocity in the numerical stage. Also, the equations related to turbulent kinetic energy and momentum by the second-order upwind discretization. The commercial software package of CFX-18 has been employed for the computational simulations (the residual error of 0.0001 is considered for justifying the convergence).
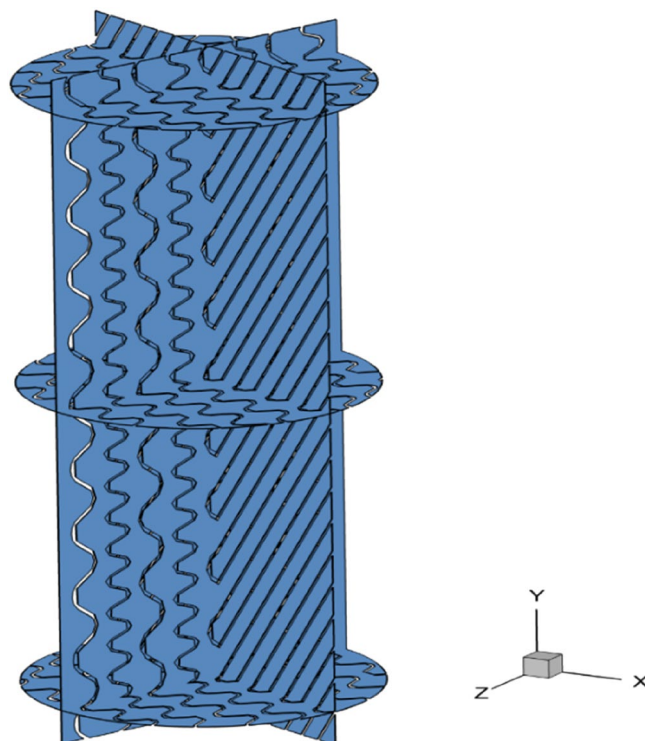
Figure 1. The simulated geometries of the PACK-1300XY.

Packing ID	a_p (1/m)	Void fraction (–)	Corrugation Specification	
			Angle	Height (mm)
PACK-1300XY	1300	0.91	45° and 60°	2

Table 1. Key structural features of the PACK-1300XY during the simulation analyses.

Element size (mm)	0.1	0.2	0.3	0.4
HETP (cm)	7.30	7.36	7.60	8.12

Table 2. Dependency of the HETP on the element size during the simulation analyses.

| System	$\rho_L\,(\mathrm{kg/m^3})$	$\mu_L\,(\mathrm{Ns/m^2})$	$D_L\,(\mathrm{m^2/s})$	$\rho_G\,(\mathrm{kg/m^3})$	$\mu_G\,(\mathrm{Ns/m^2})$	$D_G\,(\mathrm{m^2/s})$	σ (N/m)
Isopropanol/methanol	771	0.00033	3.5×10^{-9}	1.33	0.0000106	9.6×10^{-6}	0.018

Table 3. The properties of the material (liquid density, liquid viscosity, liquid diffusion coefficient, gas density, gas viscosity, gas diffusion coefficient and surface tension) used for calculating the HETP in the binary system.

Results and discussion

Inspection of the hydrodynamics behavior. *Pressure drop, dry phase.* The dry pressure drop alongside the column is a prominent parameter[73], its effectiveness should also be considered another important characteristic to estimate the wet pressure drop. Moreover, the F-factor defined in Eq. (12) shows the loudness of gas in the packed bed.

$$F - factor = u_g = \sqrt{\rho_g} \tag{12}$$

In this study, the dry pressure drop and flow field of the considered packing (i.e., PACK-1300XY) are calculated in the steady-state mode. The results are then validated by the experimental measurements in the literature[50]. Moreover, to confirm the trustworthiness and strength of the performed numerical calculations procedure, the
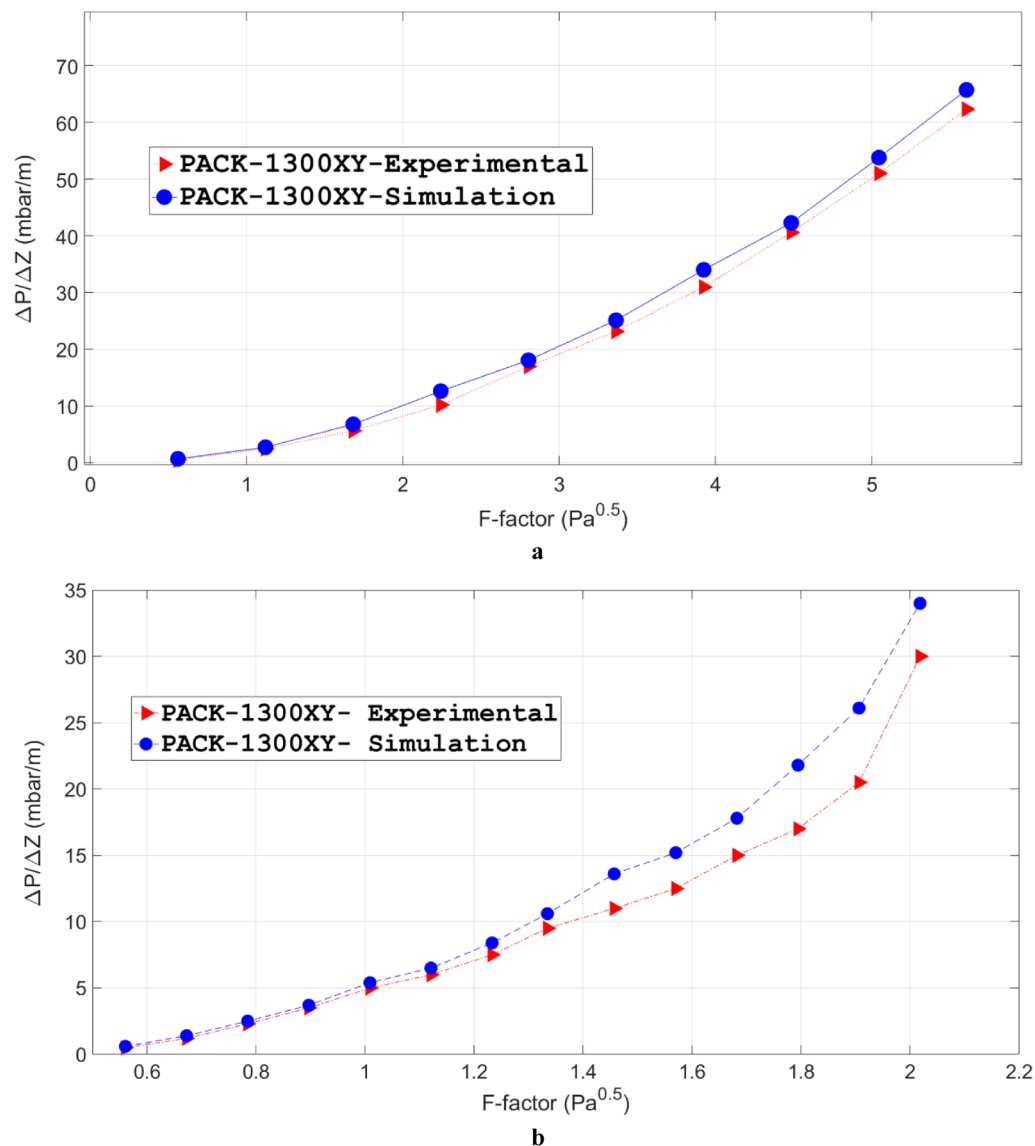
Figure 2. The experimental measurements (red triangle) and simulation results (blue circle) for the dry (**a**) and wet (**b**) pressure drop of the PACK-1300XY as a function of F-factor.

pressure drop was applied between the entry and effluent gas streams. All these criteria led to a convergence precision of 1×10^{-6} for the investigation of the velocity effect on the pressure drop. Figure 2a indicates the comparison between the simulations results and experimental measurements versus F-factor for PACK-1300XY. In addition to the good consistency between simulations and experimental results, one can observe increasing velocity for the empirical correlation and computational results when the pressure drop was increased. Moreover, the results showed a mean relative deviation of ~ 14% for the numerical findings.

As shown in Fig. 2a, due to the gas phase distribution in the whole of packings, there are always lower amounts for simulations results than the empirical values[73]. Another reason for this behavior could be related to the fact that there is a uniform distribution for the gas phase in the packed bed, which would cause a reduction for pressure drop resulting from computational works in comparison to experimental measurements.

Pressure drop, wet phase. The liquid volume fraction profile has been calculated for the binary air–water system along the packed bed and is shown in Fig. 3. This figure illustrates that the simulated structured packing has been covered with a thin layer of water. Furthermore, to better understand the relationship between the flow rate and pressure drop of gas, we compared the simulation findings and experimental measurements for the two-phase pressure drop of the binary system of air and water system, which has been provided in Fig. 2b. It could be concluded that when the rate of liquid flow increased, we observed an increasing trend in the gas pressure drop by fixing the gas velocity. This phenomenon would be explained because the decrease in the free cross-section can reduce the movement possibility of gas flow. Furthermore, the mean relative deviations between the computational results and experimental measurements were around 26% for liquid flow rate = 7.5 m³/m² h; F-factor = 1.2
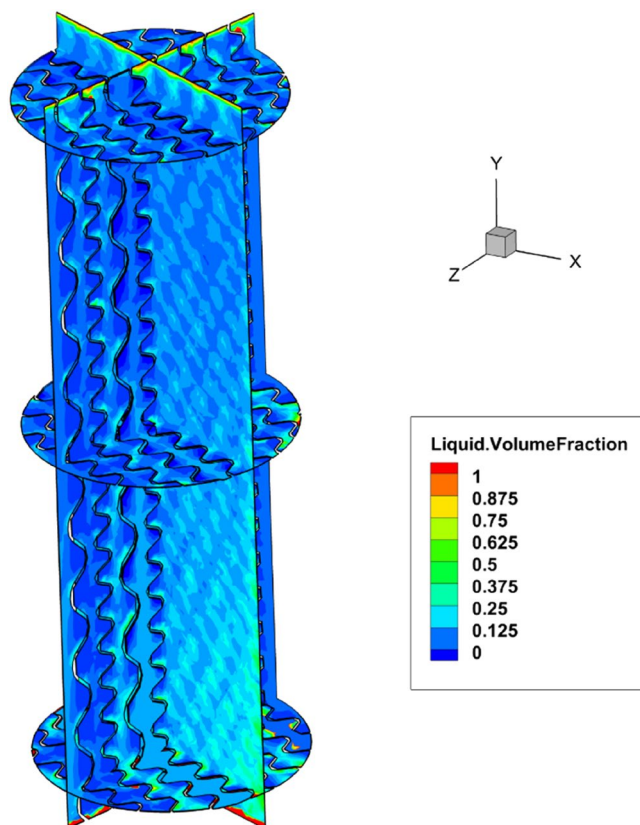
Figure 3. Liquid distribution around the PACK-1300XY obtained by the three-dimensional modeling (liquid flow rate = 7.5 m³/m² h, F-factor = 1.2 Pa$^{0.5}$).

Pa$^{0.5}$. It could also be concluded that at the higher gas velocities there is a tendency to underestimate the pressure drop for the model at the greater gas velocities. It could be clarified by a variety of chief phenomena which the key impact on the pressure drop, although these amounts have been ignored in the computational methods, including liquid back mixing, flow channeling, and rough gas/liquid-phase distribution. In conclusion, a rough flow distribution is necessary to achieve a more precise estimation for the two-phase pressure drop. The outputs of this study showed a mean relative deviation of ~ 16% for numerical data.

Based on Fig. 4 which is the distribution of the pressure around the packing, the wet pressure drop along the PACK-1300XY is ~ 190 Pa/m.

Investigating the mass transfer efficiency. As mentioned previously, the HETP parameter is an important characteristic to explain the packed column's separation efficiency[26]. Moreover, the concentration and velocity profiles along the packed bed height are needed to estimate the mass transfer efficiency of a distillation column equipped with structured packings. Therefore, it is vital to achieve the velocity distribution and the operational conditions for the calculation of the HETP[74].

Figure 5 compares the obtained mass transfer efficacy by the computational and experimental works for the PACK-1300XY. The comparison is made by monitoring the HETP of PACK-1300XY versus the gas F-factor. In addition to the expected trends of the HETP for the structured packings provided in the literature[75–77], it could be observed in Fig. 5. Moreover, there is a gradual increase for HETP from 6 to 22 cm by increasing the amounts of 0.4 to 2.1 (kg/m³)$^{0.5}$ m/s. Another finding from this figure is the difference between the computational and experimental results increased by increasing the F-factor, although there is a similar trend between them[49]. The computational results are verified by empirical findings[50] and also the HETP parameter is the major result of these trials and estimates the column height. The possibility that the mass transfer across the interface might be influenced by interfacial effects. This phenomenon could be resistant to mass transfer and affected the concentration of outlet material[39–41].

Similar to dry pressure drop behavior, there is a lower amount for computational results of HETP in various F-factor values in comparison to the empirical results[58] as presented in Fig. 5. The reason for this behavior would be related to the assumption of uniform distribution for both the liquid and gas phases in computational technique which increases the mass transfer area and consequently reduction for the HETP values and increases mass transfer rates[48,58,78]. It should be noted that the average relative deficiency of around 17% was observed for numerical data in this study.
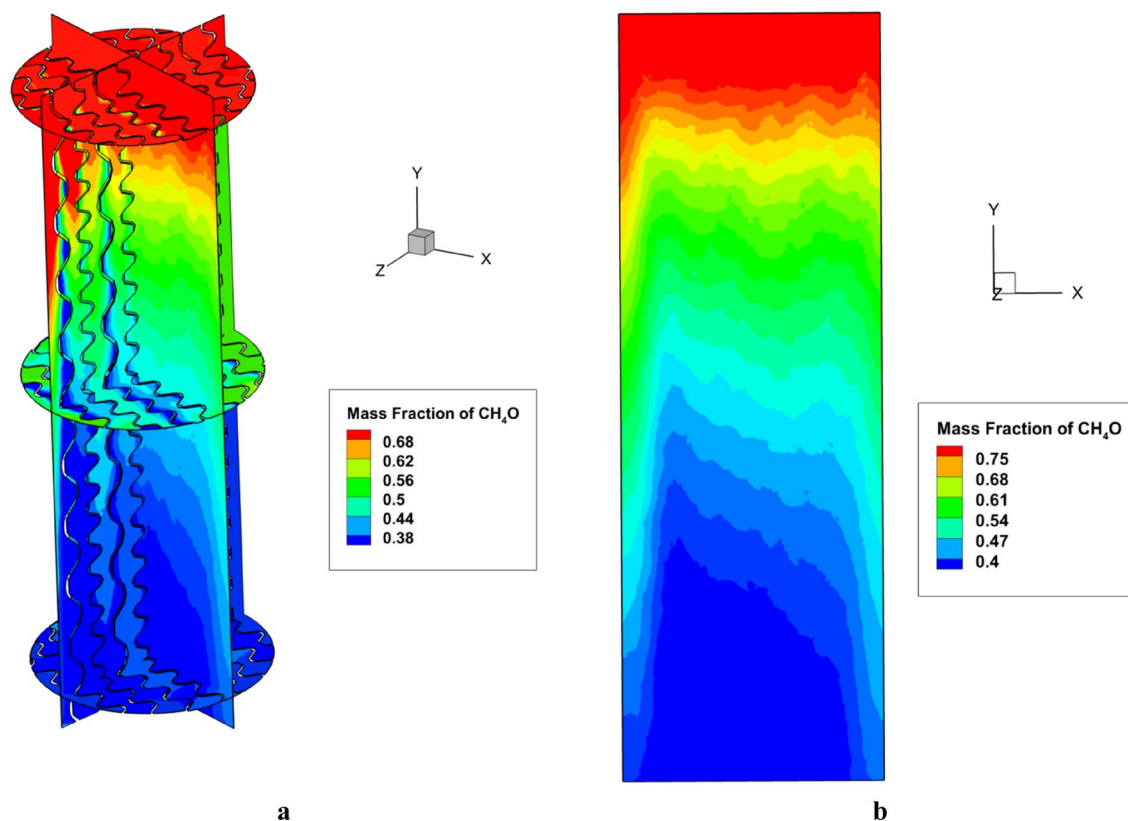
Figure 6a presents the mass fraction contour for the liquid phase of CH_3OH for the PACK-1300XY at F-factor = 1.6 m/s (kg/m³)$^{0.5}$ for different horizontal and vertical segments. Moreover, the two-dimensional mass

6
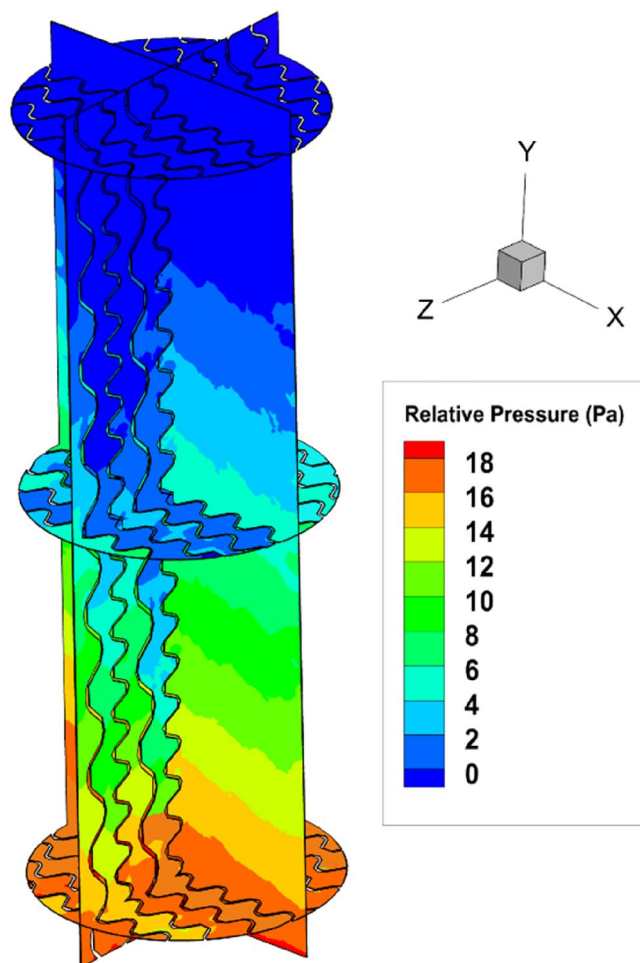
Figure 4. The pressure profile at the inside of the PACK-1300XY (F-factor = 1.2 Pa^0.5, liquid flow rate = 7.5 m³/ m² h).
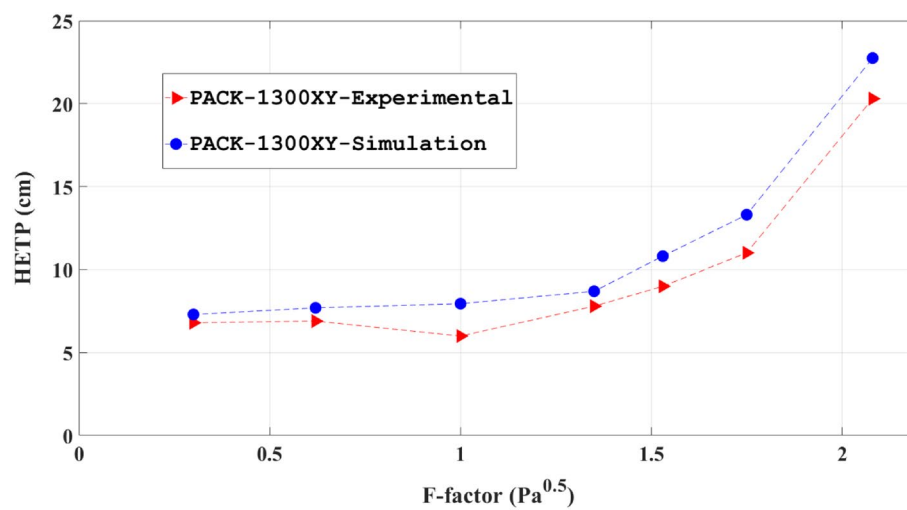
Figure 5. The experimental measurements (red triangle) and numerical predictions (blue circle) of the HETP of the PACK-1300XY.

Figure 6. (**a**) The mass fraction contour of the methanol liquid phase and (**b**) two-dimensional mass fraction contour of methanol liquid phase.

transfer contour according to the mass fraction of CH_3OH has been depicted in Fig. 6b which there is an extreme alter for the concentration of CH_3OH alongside both horizontal and vertical sections.

Conclusion

This study successfully investigated several key hydrodynamic features of the innovative wire gauze structured packing, namely PACK-1300XY applying the CFD-based simulations. The focus is concentrated on the investigation of the pressure drop (dry and wet phases), mass transfer efficiency, and height equivalent to a theoretical plate. The HETP which is an important factor for mass transfer efficiency was studied for the isopropanol/methanol system. The three-dimensional CFD simulations technique with the Eulerian–Eulerian multiphase scheme has been applied in this regard. The results approved that the mean relative deviation between the computational predictions and experimental results are around 17% (for the mass transfer efficiency), and 14% and 16% for the dry and wet pressure drop, respectively. Therefore, the simulation method could be effectively used as a reliable tool for the simulation of these devices.

References

1. Daryayehsalameh, B., Nabavi, M. & Vaferi, B. Modeling of CO2 capture ability of [Bmim][BF4] ionic liquid using connectionist smart paradigms. *Environ. Technol. Innov.* **22**, 101484 (2021).
2. Wang, H., Cui, J., Zhao, Y., Li, Z. & Wang, J. Highly efficient separation of 5-hydroxymethylfurfural from imidazolium-based ionic liquids. *Green Chem.* **23**, 405–411 (2021).
3. Chireh, M., Naseri, M. & Ghaedamini, H. Enhanced microwave absorption performance of graphene/doped Li ferrite nanocomposites. *Adv. Powder Technol.* **32**, 4697–4710 (2021).
4. Karimi, M., Shirzad, M., Silva, J. A. C. & Rodrigues, A. E. Biomass/Biochar carbon materials for CO₂ capture and sequestration by cyclic adsorption processes: A review and prospects for future directions. *J. CO₂ Util.* **57**, 101890. https://doi.org/10.1016/j.jcou.2022.101890 (2022).
5. Karimi, M. *et al.* Compost from municipal solid wastes as a source of biochar for CO₂ capture. *Chem. Engin. Technol.* **43**(7), 1336–1349. https://doi.org/10.1002/ceat.201900108 (2020).
6. Jiang, Y., Zhang, G., Wang, J. & Vaferi, B. Hydrogen solubility in aromatic/cyclic compounds: Prediction by different machine learning techniques. *Int. J. Hydrogen Energy* **46**, 23591–23602 (2021).
7. Ghanbari, S. & Vaferi, B. Experimental and theoretical investigation of water removal from DMAZ liquid fuel by an adsorption process. *Acta Astronaut.* **112**, 19–28 (2015).
8. Rahimpour, M. R., Mazinani, S., Vaferi, B. & Baktash, M. S. Comparison of two different flow types on CO removal along a two-stage hydrogen permselective membrane reactor for methanol synthesis. *Appl. Energy* **88**, 41–51 (2011).

9. Wu, X., Li, C., Zhou, Z. *et al.* Circulating purification of cutting fluid: an overview. *Int. J. Adv. Manuf. Technol.* **117**, 2565–2600. https://doi.org/10.1007/s00170-021-07854-1 (2021).
10. Karimi, M., Vaferi, B., Hosseini, S. H., Olazar, M. & Rashidi, S. Smart computing approach for design and scale-up of conical spouted beds with open-sided draft tubes. *Particuology* **55**, 179–190 (2020).
11. Karimi, M., Vaferi, B., Hosseini, S. H. & Rasteh, M. Designing an efficient artificial intelligent approach for estimation of hydrodynamic characteristics of tapered fluidized bed from its design and operating parameters. *Ind. Eng. Chem. Res.* **57**, 259–267 (2018).
12. Oduntan, O. B. & Oluwayemi, B. J. Optimization of a clay-slate fluidized bed dryer for production of fish feed. *Malays. J. Sustain. Agric.* **5**(2), 104–110 (2021).
13. Jahromi, P. F., Karimi-Sabet, J. & Amini, Y. Ion-pair extraction-reaction of calcium using Y-shaped microfluidic junctions: An optimized separation approach. *Chem. Eng. J.* **334**, 2603–2615 (2018).
14. Zhang, X.-S., Yang, G.-X., Jiang, H., Liu, W.-J. & Ding, H.-S. Mass production of chemicals from biomass-derived oil by directly atmospheric distillation coupled with co-pyrolysis. *Sci. Rep.* **3**, 1–7 (2013).
15. Abdollahi, P., Karimi-Sabet, J., Moosavian, M. A. & Amini, Y. Microfluidic solvent extraction of calcium: Modeling and optimization of the process variables. *Sep. Purif. Technol.* **231**, 115875 (2020).
16. Bravo, J. L., Rocha, J. A. & Fair, J. R. Mass transfer in gauze packings. *Hydrocarb. Process. (International Ed.)* **64**, 91–95 (1985).
17. Sadeghifar, H. Simple and rapid determination of effective Murphree component efficiencies for operating absorbers, strippers and distillation columns filled with any type of trays. *Sep. Purif. Technol.* **139**, 104–108 (2015).
18. Mohamed, A. S. A., Ahmed, M. S., Hassan, A. A. M. & Hassan, M. S. Performance evaluation of gauze packing for liquid desiccant dehumidification system, Case Stud. *Therm. Eng.* **8**, 260–276 (2016).
19. Treybal, R. E. *Mass Transfer Operations* (MCGraw-Hill, 1980).
20. Rocha, J. A., Bravo, J. L. & Fair, J. R. Distillation columns containing structured packings: a comprehensive model for their performance. 1. Hydraulic models. *Ind. Eng. Chem. Res.* **32**, 641–651 (1993).
21. Amini, Y., Karimi-Sabet, J. & Esfahany, M. N. Experimental and numerical study of multiphase flow in new wire gauze with high capacity structured packing. *Chem. Eng. Process. Process Intensif.* **108**, 35–43 (2016).
22. Dreiser, C., Gneist, G. & Bart, H. CFD-assisted characterization and optimization of the structured mass transfer packing QVF DURAPACK®. *Chem. Eng. Technol.* **36**, 545–551 (2013).
23. Suess, P. & Spiegel, L. Hold-up of Mellapak structured packings. *Chem. Eng. Process. Process Intensif.* **31**, 119–124 (1992).
24. Schultes, M. The impact of tower internals on packing performance. *Chem. Ing. Tech.* **86**, 658–665 (2014).
25. Ratheesh, S. & Kannan, A. Holdup and pressure drop studies in structured packings with catalysts. *Chem. Eng. J.* **104**, 45–54 (2004).
26. Amini, Y. & Nasr Esfahany, M. CFD simulation of the structured packings: A review. *Sep. Sci. Technol.* **54**, 2536–2554 (2019).
27. Owens, S. A., Perkins, M. R., Eldridge, R. B., Schulz, K. W. & Ketcham, R. A. Computational fluid dynamics simulation of structured packing. *Ind. Eng. Chem. Res.* **52**, 2032–2045 (2013).
28. Haroun, Y., Raynal, L. & Alix, P. Prediction of effective area and liquid hold-up in structured packings by CFD. *Chem. Eng. Res. Des.* **92**, 2247–2254 (2014).
29. Khandakar, A. & Mahmoud Salem Mohamed, A. Understanding probabilistic cognitive relaying communication with experimental implementation and performance analysis. *Sensors* **19**, 179 (2019).
30. Buchan, A. G., Yang, L. & Atkinson, K. D. Predicting airborne coronavirus inactivation by far-UVC in populated rooms using a high-fidelity coupled radiation-CFD model. *Sci. Rep.* **10**, 1–7 (2020).
31. Jayathilake, P. G., Li, B., Zuliani, P., Curtis, T. & Chen, J. Modelling bacterial twitching in fluid flows: A CFD-DEM approach. *Sci. Rep.* **9**, 1–10 (2019).
32. Gozawa, M., Takamura, Y., Aoki, T., Iwasaki, K. & Inatani, M. Computational fluid dynamics (CFD) simulation analysis on retinal gas cover rates using computational eye models. *Sci. Rep.* **11**, 1–8 (2021).
33. Anazadehsayed, A., Gerdroodbary, M. B., Amini, Y. & Moradi, R. Mixing augmentation of transverse hydrogen jet by injection of micro air jets in supersonic crossflow. *Acta Astronaut.* **137**, 403–414 (2017).
34. Khandakar, A. *et al.* Case study to analyze the impact of multi-course project-based learning approach on education for sustainable development. *Sustainability* **12**, 480 (2020).
35. Ciano, T., Ferrara, M., Babanezhad, M., Khan, A. & Marjani, A. Prediction of velocity profile of water based copper nanofluid in a heated porous tube using CFD and genetic algorithm. *Sci. Rep.* **11**, 1–12 (2021).
36. Li, H., Ju, Y., Li, L. & Xu, D. Computational fluid dynamics simulation of 13CO distillation in structured packing. *Chem. Eng. Technol.* **35**, 334–340 (2012).
37. Stephan, S. & Hasse, H. Enrichment at vapour–liquid interfaces of mixtures: establishing a link between nanoscopic and macroscopic properties. *Int. Rev. Phys. Chem.* **39**, 319–349 (2020).
38. Stephan, S., Langenbach, K. & Hasse, H. Enrichment of components at vapour–liquid interfaces: A study by molecular simulation and density gradient theory. *Chem. Eng. Trans.* **69**, 295–300 (2018).
39. Braga, C., Muscatello, J., Lau, G., Müller, E. A. & Jackson, G. Nonequilibrium study of the intrinsic free-energy profile across a liquid-vapour interface. *J. Chem. Phys.* **144**, 44703 (2016).
40. Stephan, S., Schaefer, D., Langenbach, K. & Hasse, H. Mass transfer through vapour–liquid interfaces: A molecular dynamics simulation study. *Mol. Phys.* **119**, e1810798 (2021).
41. Baidakov, V. G. & Protsenko, S. P. Molecular-dynamics simulation of relaxation processes at liquid–gas interfaces in single-and two-component lennard-jones systems. *Colloid J.* **81**, 491–500 (2019).
42. Sotoodeh, M. M., Zivdar, M. & Rahimi, R. CFD modeling of multiphase flow in reactive distillation column. *Chem. Eng. Process. Intensif.* **129**, 1–9 (2018).
43. Lappalainen, K., Gorshkova, E., Manninen, M. & Alopaeus, V. Characteristics of liquid and tracer dispersion in trickle-bed reactors: Effect on CFD modeling and experimental analyses. *Comput. Chem. Eng.* **35**, 41–49 (2011).
44. Shilkin, A., Kenig, E. Y. & Olujic, Z. Hydrodynamic-analogy-based model for efficiency of structured packing columns. *AIChE J.* **52**, 3055–3066 (2006).
45. Khandakar, A., Touati, A., Touati, F., Abdaoui, A. & Bouallegue, A. Experimental setup to validate the effects of major environmental parameters on the performance of FSO communication link in Qatar. *Appl. Sci.* **8**, 2599 (2018).
46. Olujić, Ž. Effect of column diameter on pressure drop of a corrugated sheet structured packing. *Chem. Eng. Res. Des.* **77**, 505–510 (1999).
47. Olujic, Z. Development of a complete simulation model for predicting the hydraulic and separation performance of distillation columns equipped with structured packings. *Chem. Biochem. Eng. Q.* **11**, 31–46 (1997).
48. Amini, Y., Karimi-Sabet, J., Nasr Esfahany, M., Haghshenasfard, M. & Dastbaz, A. Experimental and numerical study of mass transfer efficiency in new wire gauze with high capacity structured packing. *Sep. Sci. Technol.* **54**, 2706–2717 (2019).
49. Amini, Y., Karimi-Sabet, J. & Nasr Esfahany, M. Experimental characterization of new wire gauze with high capacity structured packing. *Can. J. Chem. Eng.* **95**, 535–542 (2017).
50. Amini, Y., Karimi-Sabet, J. & Esfahany, M. N. Characterization of new wire gauze high-capacity structured packing with varied inclination angle. *Chem. Eng. Technol.* **40**, 581–587 (2017).
51. Liu, Y. *et al.* 3D numerical simulation of a rotating packed bed with structured stainless steel wire mesh packing. *Chem. Eng. Sci.* **170**, 365–377 (2017).

52. Wu, H., Zhang, F., Zhang, Z. & Hou, L. Atomization and droplet dynamics of a gas-liquid two-phase jet under different mass loading ratios. *Int. J. Multiph. Flow.* **151**, 104043 (2022).
53. Isoz, M. & Haidl, J. Computational-fluid-dynamics analysis of gas flow through corrugated-sheet-structured packing: Effects of packing geometry. *Ind. Eng. Chem. Res.* **57**, 11785–11796 (2018).
54. Van Baten, J. M. & Krishna, R. Gas and liquid phase mass transfer within KATAPAK-S® structures studied using CFD simulations. *Chem. Eng. Sci.* **57**, 1531–1536 (2002).
55. Li, Q., Wang, T., Dai, C. & Lei, Z. Hydrodynamics of novel structured packings: An experimental and multi-scale CFD study. *Chem. Eng. Sci.* **143**, 23–35 (2016).
56. Viva, A. *et al.* Determination of liquid hold-up and flow distribution inside modular catalytic structured packings. *Chem. Eng. Res. Des.* **89**, 1414–1426 (2011).
57. Manh, T. D., Nam, N. D., Babazadeh, H. & Moradi, R. Computational fluid dynamics characterization of high-capacity structured packing. *Chem. Eng. Technol.* **43**, 1690–1698 (2020).
58. Haghshenas Fard, M. *et al.* CFD simulation of mass transfer efficiency and pressure drop in a structured packed distillation column. *Chem. Eng. Technol. Ind. Chem. Equip. Process Eng.* **30**, 854–861 (2007).
59. Hashemipour, N. *et al.* Numerical study of n-heptane/benzene separation by thermal diffusion column, Chinese. *J Chem. Eng.* **27**, 1745–1755 (2019).
60. Karbasi, E. *et al.* Experimental and numerical study of air-gap membrane distillation (AGMD): Novel AGMD module for Oxygen-18 stable isotope enrichment. *Chem. Eng. J.* **322**, 667–678 (2017).
61. Khandakar, A. *et al.* A case study to identify the hindrances to widespread adoption of electric vehicles in qatar. *Energies* **13**, 3994 (2020).
62. Amini, Y., Ghaednian-Jahromi, A., Karimi-Sabet, J., Dastbaz, A. & Hassanvand, A. CFD simulation of He/CH4 separation by Hyflon AD60X membrane. *Chem. Biochem. Eng. Q.* **35**, 355–367 (2021).
63. Raynal, L., Boyer, C. & Ballaguet, J. Liquid holdup and pressure drop determination in structured packing with CFD simulations. *Can. J. Chem. Eng.* **82**, 871–879 (2004).
64. Wilcox, D. C. *Turbulence Modeling for CFD* (DCW Industries, 1998).
65. Chowdhury, M. E. H. *et al.* Design, construction and testing of iot based automated indoor vertical hydroponics farming test-bed in qatar. *Sensors* **20**, 5637 (2020).
66. Nikou, M. R. K. & Ehsani, M. R. Turbulence models application on CFD simulation of hydrodynamics, heat and mass transfer in a structured packing. *Int. Commun. Heat Mass Transf.* **35**, 1211–1219 (2008).
67. Salimi, H., Hashemipour, N., Karimi-Sabet, J. & Amini, Y. Appling the computational fluid dynamics studies of the thermogravitational column for N2-CO2 and He–Ar gas mixtures separation. *Chem. Prod. Process Model.* **35**, 355–367 (2021).
68. Hashemipour, N. *et al.* Experimental and simulation investigation on separation of binary hydrocarbon mixture by thermogravitational column. *J. Mol. Liq.* **268**, 791–806 (2018).
69. Edalatpour, A., Hassanvand, A., Gerdroodbary, M. B., Moradi, R. & Amini, Y. Injection of multi hydrogen jets within cavity flameholder at supersonic flow. *Int. J. Hydrogen Energy.* **44**, 13923–13931 (2019).
70. Amini, Y., Mokhtari, M., Haghshenasfard, M. & Gerdroodbary, M. B. Heat transfer of swirling impinging jets ejected from Nozzles with twisted tapes utilizing CFD technique, Case Stud. *Therm. Eng.* **6**, 104–115 (2015).
71. Yankova, G., Tur, D., Parshin, D., Cherevko, A. & Akulov, A. Cerebral arterial architectonics and CFD simulation in mice with type 1 diabetes mellitus of different duration. *Sci. Rep.* **11**, 1–9 (2021).
72. Manh, T. D., Nam, N. D., Babazadeh, H. & Moradi, R. Characterization of new wire gauze-structured packing: Experimental study. *Chem. Eng. Technol.* **43**, 2469–2476 (2020).
73. Amini, Y., Karimi-Sabet, J. & Esfahany, M. N. Experimental and numerical simulation of dry pressure drop in high-capacity structured packings. *Chem. Eng. Technol.* **39**, 1161–1170 (2016).
74. Billet, R. & Schultes, M. Predicting mass transfer in packed columns. *Chem. Eng. Technol. Ind. Chem. Equip. Process Eng.* **16**, 1–9 (1993).
75. Lautenschleger, A., Olenberg, A. & Kenig, E. Y. A systematic CFD-based method to investigate and optimise novel structured packings. *Chem. Eng. Sci.* **122**, 452–464 (2015).
76. Olujić, Ž & Seibert, A. F. Predicting the liquid phase mass transfer resistance of structured packings. *Chem. Biochem. Eng. Q.* **28**, 409–424 (2014).
77. Wang, C., Perry, M., Rochelle, G. T. & Seibert, A. F. Packing characterization: Mass transfer properties. *Energy Procedia.* **23**, 23–32 (2012).
78. Haroun, Y., Legendre, D. & Raynal, L. Volume of fluid method for interfacial reactive mass transfer: Application to stable liquid film. *Chem. Eng. Sci.* **65**, 2896–2909 (2010).

Acknowledgements

Author contributions

All authors contributed equally.

Competing interests

The authors declare no competing interests.

Additional information

Correspondence and requests for materials should be addressed to H.A.D. or B.V.

Reprints and permissions information is available at www.nature.com/reprints.

Publisher's note Springer Nature remains neutral with regard to jurisdictional claims in published maps and institutional affiliations.